

New observational limits on dark radiation in brane-world cosmology

Nishanth Sasanka,* Mayukh Raj Gangopadhyay,† Grant J Mathews,‡ and Motohiko Kusakabe§

*Center for Astrophysics, Department of Physics,
University of Notre Dame, Notre Dame, IN 46556*

(Dated: November 24, 2021)

A dark radiation term arises as a correction to the energy momentum tensor in the simplest five-dimensional RS-II brane-world cosmology. In this paper we revisit the constraints on dark radiation based upon the newest results for light-element nuclear reaction rates, observed light-element abundances and the power spectrum of the Cosmic Microwave Background (CMB). Adding dark radiation during big bang nucleosynthesis alters the Friedmann expansion rate causing the nuclear reactions to freeze out at a different temperature. This changes the final light element abundances at the end of BBN. Its influence on the CMB is to change the effective expansion rate at the surface of last scattering. We find that our adopted BBN constraints reduce the allowed range for dark radiation to between -12.1% and $+6.2\%$ of the ambient background energy density. Combining this result with fits to the CMB power spectrum, the range decreases to -6.0% to $+6.2\%$. Thus, we find, that the ratio of dark radiation to the background total relativistic mass energy density ρ_{DR}/ρ is consistent with zero although in the BBN analysis there could be a slight preference for a negative contribution. However, the BBN constraint depends strongly upon the adopted primordial helium abundance.

PACS numbers: 98.80.Cq, 26.35.+c, 98.80.Ft, 98.70.Vc

I. INTRODUCTION

One of the proposed solutions to the hierarchy problem among the fundamental forces is the introduction of compact extra dimensions. However, this creates a new hierarchy problem between the weak forces and the size of the compact extra dimensions. A possible solution was suggested by Randall and Sundrum [1] by introducing a non-compact large extra dimension. In that model, the observed universe is a four-dimensional spacetime embedded in a five-dimensional anti-de-sitter space (AdS5).

The projected three-space Friedmann equation of the five dimensional universe reduces to [2]:

$$\left(\frac{\dot{a}}{a}\right)^2 = \frac{8\pi G_N}{3}\rho - \frac{K}{a^2} + \frac{\Lambda_4}{3} + \frac{\kappa_5^4}{36}\rho^2 + \frac{\mu}{a^4} . \quad (1)$$

Here $a(t)$ is the usual scale factor for the three-space at time t , while ρ is the energy density of matter in the normal three space. G_N is the four dimensional gravitational constant and is related to its five dimensional counterpart κ_5 by

$$G_N = \kappa_5^4 \lambda / 48\pi , \quad (2)$$

where λ is the intrinsic tension on the brane and $\kappa_5^2 = M_5^{-3}$, with M_5 the five dimensional Planck mass. The Λ_4 in the third term on the right-hand side is the four dimensional cosmological constant and is related to its

five dimensional counterpart by

$$\Lambda_4 = \kappa_5^4 \lambda^2 / 12 + 3\Lambda_5 / 4 . \quad (3)$$

Note that for Λ_4 to be close to zero, Λ_5 should be negative. Hence the spacetime is AdS5.

In standard Friedmann cosmology only the first three terms arise. The fourth term is probably negligible during most of the radiation dominated epoch since ρ^2 decays as a^{-8} in the early universe. However this term could be significant during the beginning of the epoch of inflation [3–5].

The last term is the dark radiation [6, 7]. It is called radiation since it scales as a^{-4} . It is a constant of integration that arises from the projected Weyl tensor describing the effect of graviton degrees of freedom on the dynamics of the brane. One can think of it, therefore, as a projection of the curvature in higher dimensions. In principle it could be either positive or negative.

Although it is dubbed dark radiation it is not related to relativistic particles. Since it does not gravitate, flow or scatter as would a light neutrino species, its effects on the cosmic microwave background (CMB) is different than that of normal radiation. Nevertheless, since it scales like radiation, its presence can alter the expansion rate during the radiation dominated epoch. This effect has been studied previously by several authors [8, 9]. Here we update those previous studies in the context of newer constraints on light elemental abundances, BBN nuclear reaction rates and the CMB.

II. EFFECTS OF DARK RADIATION

Dark radiation can have significant effects on the light element abundances produced during big bang nucle-

*nsasanka@nd.edu

†mgangopa@nd.edu

‡gmathews@nd.edu

§mkusakab@nd.edu

osynthesis (BBN). It also affects the angular power spectrum of the CMB. Altering the expansion rate changes the temperature at which various nuclear reactions freeze out. This leads to deviations in the final BBN light element abundances. In this paper we define $\rho_{DR} \equiv (3/8\pi G_N)\mu/a^4$ as the energy density of the dark radiation, and parametrize ρ_{DR}/ρ to be the ratio of the energy density of the dark radiation to the total energy density in relativistic particles at 10 MeV (before $e^+ - e^-$ annihilation). The corresponding changes in the BBN abundances and the CMB power spectrum are then computed.

Observations of the CMB and the Hubble expansion rate H_0 suggests the possible existence of an additional density in the form of dark radiation [10, 11]. The effect of the altered expansion rate on BBN was first discussed by [12]. This effect was further studied by many authors [13–15]. We note, however, that exotic relativistic particles that do not interact with normal background particles have also been referred to as dark radiation. However, they are not the same as the dark radiation discussed here. The effects of these exotic particles have been studied by numerous authors [16–18].

The effect of an altered expansion rate during the epoch of BBN and CMB has been studied in the context of constraining the effective number of neutrino species N_{eff} [15, 19–27]. Positive and negative dark radiation can be associated with the uncertainty in the number of neutrino species ΔN_ν . The standard model suggests that we have 3 types of neutrinos, therefore we assume this to be true during the epoch of BBN. An addition of dark radiation (ρ_{DR}) can be related to a corresponding value in ΔN_ν given by.

$$\left(\sum_{i=e,\mu,\tau} \rho_{\nu_i} \right) + \rho_{DR} \equiv (3 + \Delta N_\nu)\rho_{\nu_e} \equiv N_{eff}\rho_{\nu_e} \quad , \quad (4)$$

where ρ_{ν_i} corresponds to the sum over neutrino plus anti-neutrino energy densities

$$\rho_{\nu_i} = 2 \frac{7}{8} \frac{\pi^2}{30} T_{\nu_i}^4 \quad , \quad (5)$$

where T_{ν_i} is the temperature of each neutrino species. Note, that since each neutrino species is slightly heated by the e^+e^- annihilation before it decouples at a different temperature, $\Delta N_\nu = 0.046$ even in the standard big bang.

The dark radiation arising from the RS model is different from the other possible "dark" relativistic particles (e.g. sterile neutrinos). Indeed, during the BBN epoch the dark radiation in the RS model is nearly equivalent to an effective neutrino species. However it acts differently on the CMB. Whereas light neutrinos or non-interacting particles can stream and gravitate, a dark radiation term remains uniform everywhere. Thus, as clarified below, there is a cosmological sensitivity to either relativistic or light neutrinos at the CMB epoch, particularly given the fact that their number density is comparable to that

of CMB photons. A dark radiation term of the form of interest here, however, has a different effect on the CMB.

This high density of free streaming particles can inhibit the growth of structure at late times, leading to changes in large scale structure (LSS) that can be constrained by the CMB and matter power spectrum. In particular, the number of neutrino species primarily affects the CMB by altering the photon diffusion (Silk damping) scale relative to the sound horizon. The sound horizon sets the location of the acoustic peaks while photon diffusion suppresses power at small angular scales. This affects both the ISW effect and the look back time. Hence, the effect of RS dark radiation is not equivalent to adding ΔN_ν neutrino species. Moreover, if the added neutrino has a light mass, the CMB constrains that mass through its effect on structure growth in two ways: 1) the early Integrated Sachs Wolfe (ISW) effect, and 2) gravitational lensing of the CMB by LSS. Indeed, A significant fraction of the power in the CMB on large angular scale is from the early ISW effect, but unaffected by the RS dark radiation of interest here. Hence, the CMB constraints on the dark radiation discussed here are not equivalent to the constraints on ΔN_ν deduced in the *Planck* cosmological parameters paper [28].

Although the Planck cosmological parameters paper [28] mentions dark radiation, they use that term in the sense of a non-interacting or massless particle, not as the effect of higher dimensional curvature. Hence, "dark radiation" was treated as an effective neutrino species. Similarly, the recent review of Cyburt et al [19] does not mention dark radiation. Although a number of papers in our scan the literature mention the term dark radiation, they invariably refer to an extra relativistic species that can be treated as an effective number of neutrinos, not the effect of curvature in extra dimension. Similarly, although there are many references to the extra-dimensional dark radiation term in the literature, there has been no treatment of the combined BBN and CMB constraints since [8]. Hence, there is a need to revisit this issue in light of the recent Planck results and revised light element abundance constraints.

III. BBN CONSTRAINT

The light element abundances present at the end of BBN can be used to constrain the physical conditions during the nucleosynthesis epoch. We use a standard BBN code [29] with a number of reaction rates updated [30]. We also replaced the modified Bessel function approximation with a more accurate Fermi-integral solver and checked for any differences in the final abundances. The primordial helium abundance (Y_p) is deduced from HII regions in metal poor irregular galaxies extrapolated to zero metallicity [19]. We adopt $Y_p = 0.2449 \pm 0.0040(2\sigma)$ from [19].

Deuterium is measured from the spectra of Lyman-alpha absorption systems in the foreground of high red-

shift QSOs. A two sigma region of

$$2.45 \times 10^{-5} \leq D/H \leq 2.61 \times 10^{-5} \quad (6)$$

is adopted from [19].

The inclusion of positive dark radiation implies extra energy density during BBN. Its effects has been studied by many authors [31–33]. Positive dark radiation increases the cosmic expansion rate and causes the nuclear reactions to freeze out at a higher temperature. As a result, the neutron to proton ratio increases, since the n/p ratio is related to a simple Boltzmann factor at freezeout

$$n/p = \exp(-\Delta m/T) \quad , \quad (7)$$

where $\Delta m = 1.293$ MeV is the neutron-proton mass difference, and T is the photon temperature. The increased neutron mass fraction from a positive dark radiation term increases the D/H and Y_p abundances. In addition, the faster cosmic expansion results in the freezeout of the deuterium destruction via the reactions ${}^2\text{H}(d,n){}^3\text{He}$ and ${}^2\text{H}(d,p){}^3\text{H}$ at a higher temperature. This also leads to a larger deuterium abundance. The abundances of ${}^3\text{H}$ and ${}^3\text{He}$ are larger for a positive dark radiation. This is because these nuclides are mainly produced via the reactions ${}^2\text{H}(d,n){}^3\text{He}$ and ${}^2\text{H}(d,p){}^3\text{H}$, respectively, and the deuterium abundance is higher. When the dark radiation is negative the opposite effect occurs.

The primordial ${}^7\text{Li}$ abundance is deduced from the observed abundances in low mass metal poor stars. For ${}^7\text{Li}$ we adopt the 2σ constraint of [19]

$$1.00 \times 10^{-10} \leq {}^7\text{Li}/\text{H} \leq 2.20 \times 10^{-10} \quad . \quad (8)$$

There is a well known lithium problem [19] whereby the predicted primordial lithium abundance exceeds the observed primordial lithium abundance by about a factor of 3 for $\eta = (6.10 \pm 0.04) \times 10^{-10}$ deduced from the *Planck* analysis [28] of the CMB primordial power spectrum.

Figure 1 shows the calculated light element abundances, Y_p , D/H , ${}^3\text{He}/\text{H}$, and Li/H as a function of η . The solid green line is the result for the standard BBN with no dark radiation. The dot dashed black line and the dashed blue line show the results of BBN in which the energy densities of the dark radiation are +6.2% and -12.1%, respectively, of the total particle energy density. The two lines correspond to the cases of the upper and lower limits on ρ_{DR} derived from the constraints on light element abundances. The vertical solid blue lines enclose the $\pm 1\sigma$ constraint on η [28]. The horizontal lines correspond to the observational upper and lower limits on primordial abundances.

For the case of positive dark radiation, we find a decrease of the ${}^7\text{Li}$ abundance for $\eta \lesssim 3 \times 10^{-10}$ and an increase for $\eta \gtrsim 3 \times 10^{-10}$. We note that the primordial ${}^7\text{Li}$ nuclei are produced as ${}^7\text{Li}$ in the low η region and ${}^7\text{Be}$ in the high η region during BBN. A positive dark radiation term leads to a slight excess of the ${}^7\text{Li}$ abundance

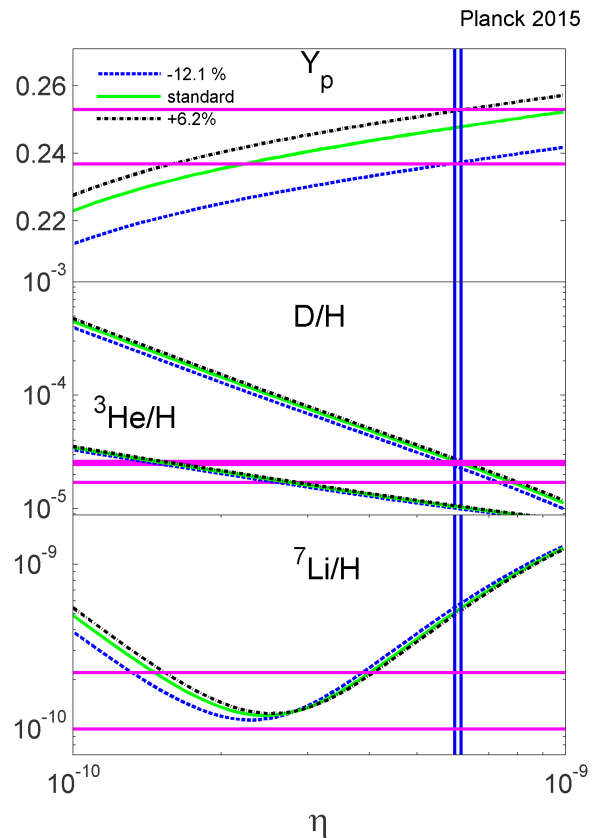


FIG. 1: (Color online) Light element abundances, Y_p , D/H , ${}^3\text{He}/\text{H}$, and Li/H as a function of baryon to photon ratio η . The red horizontal lines correspond to the adopted observational upper and lower limits on primordial abundances. The solid green line is the result for the standard BBN with no dark radiation. The dot dashed black line and the dashed blue line show the results of BBN in which the energy densities in dark radiation are +6.2% and -12.1%, respectively, of the total relativistic particle energy density (at 10 MeV). The two lines correspond to upper and lower limits on ρ_{DR} derived from the constraints on light element abundances. The vertical solid blue lines show the CMB constraint on η from *Planck* [28].

because ${}^7\text{Li}$ is produced via the ${}^4\text{He}(t,\gamma){}^7\text{Li}$ reaction and the abundance of ${}^3\text{H}$ is higher. There is also less time for the lithium destruction reaction ${}^7\text{Li}(p,\alpha){}^4\text{He}$. On the other hand, a positive dark radiation decreases the ${}^7\text{Be}$ abundance. The slight increase in the ${}^3\text{He}$ abundance results in a somewhat increased production rate of ${}^7\text{Be}$ via the reaction ${}^4\text{He}({}^3\text{He},\gamma){}^7\text{Be}$. However, the significant increase of the neutron abundance leads to an enhanced destruction rate of ${}^7\text{Be}$ via the reaction ${}^7\text{Be}(n,p){}^7\text{Li}$. As a result, the final ${}^7\text{Be}$ abundance decreases. In either case, dark radiation does not affect the primordial lithium abundance sufficiently to solve the lithium problem without violating the ${}^4\text{He}$ and deuterium constraints. Hence, we presume that the lithium problem is solved by another means and do not utilize the ${}^7\text{Li}$ abundance as a

constraint on dark radiation.

We estimate the likelihood for ρ_{DR}/ρ assuming a gaussian prior on the observational limits of D/H and Y_p . We define the marginalized likelihood function by

$$L(\rho_{DR}/\rho) = \int_{\eta} L_{D/H} L_{Y_p} d\eta \quad (9)$$

where

$$L_i = \frac{1}{\sqrt{2\pi}\sigma_i} \exp \left\{ -\frac{[Y_{i,BBN}(\rho_{DR}/\rho, \eta) - Y_{i,obs}]^2}{2\sigma_i^2} \right\} \quad (10)$$

The L_D and L_{Y_p} are the likelihood values we obtain from the deuterium and helium abundances. $Y_{i,BBN}$ is the yield calculated by the BBN code and $Y_{i,obs}$ is the observational abundance. σ_i is the uncertainty of the observational abundances. Here i can be either D/H or Y_p . A plot of the Gaussian fit to the likelihood values for ρ_{DR}/ρ is given in Figure 2.

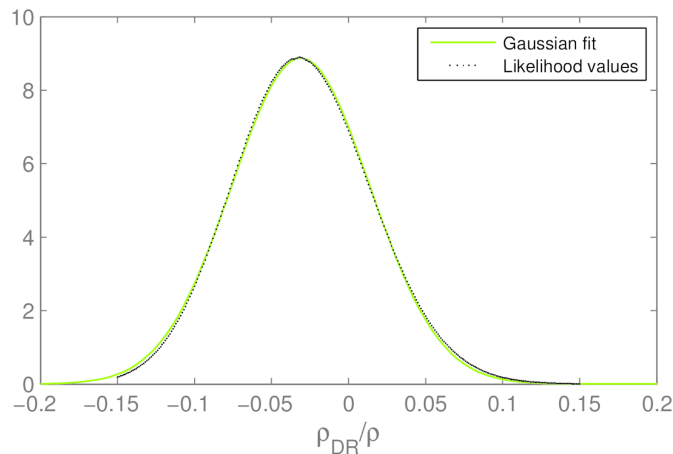


FIG. 2: Likelihood function for ρ_{DR}/ρ (black line), with a Gaussian distribution (green line)

We obtain 1- σ bound on ρ_{DR}/ρ of $(-3.10 \pm 4.49 \%)$. This corresponds to N_{eff} in the range of 2.81 ± 0.28 , or in terms of an equivalent number of neutrino species, via Eq. (4) we have $\Delta N_{\nu} = -0.19 \pm 0.28$. This is comparable to the BBN+ Y_p +D value of $N_{eff} = 2.85 \pm 0.28$ deduced in Ref. [19].

IV. CMB CONSTRAINTS

Although the epoch of photon last scattering is in the matter dominated epoch, there remains an effect on the CMB power spectrum due to the still significant contribution from relativistic mass energy and the effect of the uniform dark radiation term on the expansion rate and acoustic oscillations of the cosmic fluid. On the other hand, the CMB power spectrum is very sensitive to a

number of other parameters that have little or no effect on BBN. Thus, to obtain a total constraint on the dark radiation contribution to energy density, we have performed a simultaneous fit to the TT power spectrum of temperature fluctuations in the CMB. To achieve this, we have fixed most of the cosmological parameters to their optimum values [28] and only varied the dark radiation content and η in the fit. Fits were made to the *Planck* data [28] using the CAMB code [34]. In the limit of no dark radiation we recover the *Planck* value of $\eta = (6.10 \pm 0.04) \times 10^{-10}$ (1σ) [28]. For η fixed by the *Planck* analysis, the 2σ constraint from the CMB alone would imply $-9.0 \% < \rho_{DR}/\rho < 13.5 \%$.

We note, however, that the deduced dark radiation content is sensitive to the adopted value of H_0 . In the present work we utilize $H_0 = 66.93 \pm 0.62 \text{ km s}^{-1} \text{ Mpc}^{-1}$ (Planck+BAO+SN) from the *Planck* analysis [28]. However, a larger value is preferred [35] from local measurements of H_0 , and a larger value of $H_0 = 73.24 \pm 1.74 \text{ km s}^{-1} \text{ Mpc}^{-1}$ was obtained [28] when adding a prior on H_0 . Adopting this larger value would shift the inferred dark radiation constraint toward larger positive values. We prefer the lower value of H_0 deduced by *Planck* because this discrepancy between the local value and the CMB value would in fact be explained [35] by the presence of dark radiation at the CMB epoch.

It is important to appreciate that adding a dark radiation term is not equivalent to adding an effective number of neutrino species to the CMB analysis. This is illustrated in Figure 3. The upper and lower panels of Figure 3 show the effects on the CMB TT power spectrum of adding dark radiation vs. an effective number of neutrino species, respectively. This figure plots the usual normalized amplitude C_l of the multipole expansion for the TT power spectrum as a function of the moment l . As can be seen on the upper figure, a positive dark radiation has only a slight effect, while a negative dark radiation term (red line) slightly increases the amplitude of the acoustic peaks due to the diminished expansion rate. However, a relativistic neutrino-like species can stream and gravitate. Therefore, it has the opposite effect of increasing the amplitude of the first acoustic peak for a positive contribution while decreasing the amplitude for a negative contribution. In addition, a relativistic species also shifts the location of the higher harmonics. Thus, it is important to re-examine the CMB constraints on the brane-world dark radiation term independently of any previously derived constraints on the effective number of neutrino species.

Figure 4 shows the combined constraints on η vs. dark radiation based upon our fits to both BBN and the CMB power spectrum. The contour lines on Figure 4 show the CMB 1, 2, and 3σ confidence limits in the η vs. dark radiation plane. The shaded regions show the BBN Y_p and D/H constraints as labeled.

The best fit concordance shown in Figure 4 is consistent with no dark radiation although in the BBN analysis there is a slight preference for negative dark radi-

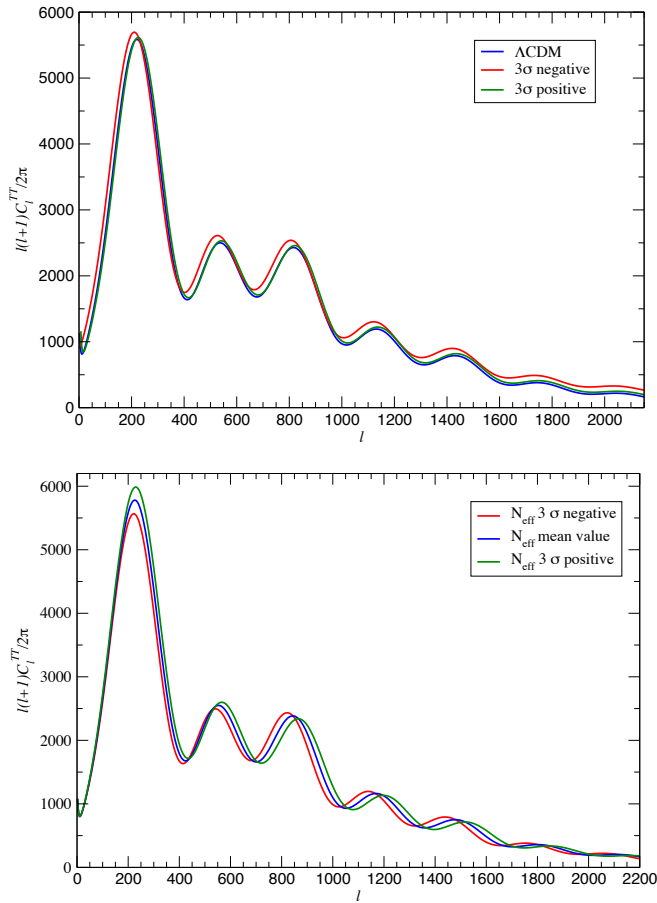


FIG. 3: (Color online) Upper panel illustrates the effect of Dark Radiation on fits to the TT CMB power spectrum. Lines drawn indicate the $\pm 3\sigma$ deviations in the BBN constraint as labeled. Lower panel shows the equivalent BBN $\pm 3\sigma$ constraints, but in this case it is treated as an effective number of neutrino species. Clearly the effect of dark radiation on the CMB is different than an equivalent number of neutrino species.

ation. A similar result was found in the previous analysis of Ref. [8]. However, the magnitude of any dark radiation is much more constrained in the present analysis. This can be traced to both the CMB and new light-element abundances. Also, it is worth mentioning that the value of η deduced from the WMAP data is $(6.19 \pm 0.14) \times 10^{-10}$, while the (WMAP+ BAO + H_0) data is $(6.079 \pm 0.09) \times 10^{-10}$ [36]. Hence, the BBN dark radiation constraint based upon the WMAP results would be nearly identical and would also have a slight preference for a negative dark radiation.

We note, however, that the results in Figure 4 are sensitive to the the value of $Y_P = 0.2449 \pm 0.0040$ adopted from Ref. [19] based upon the recent primordial helium abundance determinations from Aver, Olive, and Skillman [37]. This result is based on data from Izotov and collaborators [38]. However, using data that overlaps strongly with that of Ref. [37], a higher helium abun-

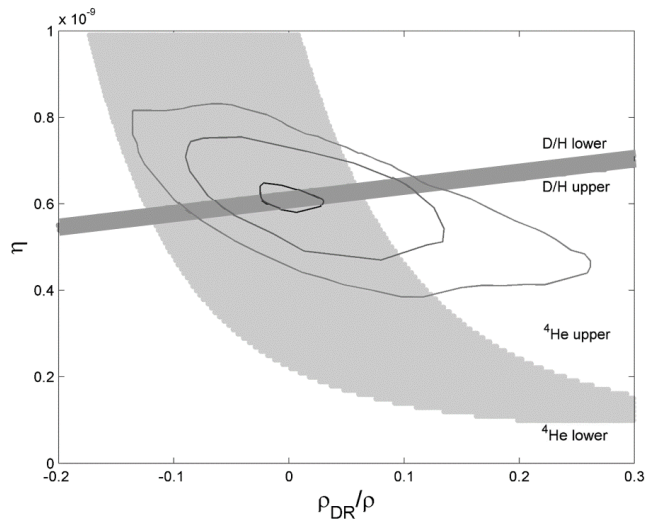


FIG. 4: (Color online) Constraints on dark radiation in the ρ_{DR}/ρ vs. η plane. Contour lines show the 1, 2, and 3 σ confidence limits based upon our fits to the CMB power spectrum. Dark shaded lines show the constraints from the primordial deuterium abundance as described in the text. The light shaded region shows the Y_P constraint.

dance of $Y_P = 0.2551 \pm 0.0022$ was deduced in [38]. If we adopt the larger value for the helium abundance then the 2 σ BBN constraint on the dark radiation content increases from to positive values of $+3.2\% < \rho_{\text{DR}}/\rho < 14.4\%$. Nevertheless we prefer the Bayesian analysis of [37] as it arguably incorporates a better treatment of correlated errors. It is also more consistent with the CMB constraint.

V. CONCLUSION

In conclusion we deduce that based upon our adopted 2 σ (95% C. L.) BBN constraints, brane-world dark radiation is allowed in the range of -12.1% to $+6.2\%$ ($\Delta N_\nu = -0.19 \pm 0.56$) compared to the range deduced in Ref. [8] of -123% to 10.5% based upon constraints available at the time of that paper. After taking into account the 2 σ limits on the dark radiation from the fit to the CMB power spectrum, this region shrinks to a range of -6.0% to $+6.2\%$ ($\Delta N_\nu = -0.19^{+0.56}_{-0.18}$). However, if the higher helium abundance of [38] were adopted, the allowed range increases to The 1 σ BBN constraint ($2.63 \leq N_\nu \leq 3.38$, $\Delta N_\nu = -0.19 \pm 0.28$) is comparable to the values deduced by [19, 28]. For η fixed by the *Planck* analysis, the constraint on positive dark radiation comes from the upper bound on the ^4He mass fraction and the upper bounds on the D/H. The limit on negative dark radiation arises from the constraint on cosmic expansion rate at the epoch of last scattering (the CMB) and the lower bound of D/H.

We caution, however, that either a larger value for the

Hubble parameter [35] could shift the allowed CMB range (or a larger primordial helium abundance [38] could shift the BBN range) to a higher positive contribution of dark radiation. For example, if the higher helium abundance of [38] were adopted, the allowed range increases to $+3.2\% < \rho_{\text{DR}}/\rho < 13.5\%$. In this case the lower bound is from BBN and the upper bound is from the CMB.

We also checked the corresponding ${}^7\text{Li}/\text{H}$ abundance for the allowed ranges of dark radiation. For dark radiation of $+6.2\%$ and η of 6.1×10^{-10} the lithium abundance is 5.19×10^{-10} slightly alleviating the lithium problem. The 3σ CMB contour combined with D/H corresponds to a lower limit of dark radiation of -9.1% . In this case the corresponding lithium abundance is increased to

5.64×10^{-10} exacerbating the lithium problem. Hence, although a positive dark radiation slightly reduces the lithium abundance, it is not sufficient to solve the lithium problem.

Acknowledgments

Work at the University of Notre Dame is supported by the U.S. Department of Energy under Nuclear Theory Grant DE-FG02-95-ER40934. One of the authors (MK) acknowledges support from the JSPS.

-
- [1] L. Randall and R. Sundrum, Phys. Rev. Lett. **83**, 3370 (1999); **83**, 4690 (1999).
 - [2] D. Langlois, Phys. Rev. Lett. **86** 2212, (2001); Phys. Rev. **D62**, 126012 (2000).
 - [3] R. Maartens, D. Wands, B. A. Bassett, and I. P. C. Heard, Phys. Rev. **D62** 041301 (2000)
 - [4] N. Okada and S. Okada, Int. J. Mod. Phys, **A31**, 1650078 (2016)
 - [5] M. R. Gangopadhyay and G. J. Mathews, JCAP, Submitted (2016), ArXiv: 1611.50123 hep/ph
 - [6] P. Binetruy, C. Deffayet, U. Ellwanger, and D. Langlois, Phys. Lett. **B477**, 285 (2000)
 - [7] S. Mukohyama, Phys. Lett. **B473**, 241 (2000).
 - [8] K. Ichiki, M. Yahiro, T. Kajino, M. Orito and G. J. Mathews Phys. Rev. **D66**, 043521 (2002).
 - [9] J. D. Bratt, A. C. Gault, R. J. Scherrer, and T. P. Walker, Phys. Lett. **B546**, 19 (2002).
 - [10] C. Cheng, Q.-G. Huang, Phys. Rev. **D 89**, 043003 (2014).
 - [11] E. Calabrese, M. Archidiacono, A. Melchiorri, and B. Ratra, Phys. Rev. **D86** 043520 (2012).
 - [12] F. Hoyle and R. J. Taylor, *Nature* **203**, 1108 (1964)
 - [13] V. F. Shvartsman, ZhETF Pis ma Redaktsiiu, **9**, 315 (1969); JETP Lett., **9**, 184 (1969).
 - [14] P. J. E. Peebles, Astrophys. J. **146** 542 (1966).
 - [15] G. Steigman, D. N. Schramm, J. E. Gunn, Phys. Lett. **B66**, 202 (1977).
 - [16] J. L. Menestrina and R. J. Scherrer, Phys. Rev. **D85**, 047301 (2012).
 - [17] G. Steigman, Phys. Rev. **D87**, 103517 (2013).
 - [18] K. M. Nollett and G. Steigman, Phys. Rev. **D91**, 083505 (2015).
 - [19] R. H. Cyburt, B. D. Fields, K. A. Olive, and T-H. Yeh Rev. Mod. Phys. **88**, 015004 (2016).
 - [20] M. Cicoli, J. P. Conlon and F. Quevedo, Phys. Rev. **D87** 043520 (2013).
 - [21] A. M. Boesgaard, G. Steigman, Ann. Rev. Astr. Astrophys., **23**, 319 (1985).
 - [22] G. Steigman, Advances in High Energy Physics, **2012**, 268321 (2012).
 - [23] K. Nollett and G. Holder, arXiv:1112.2683
 - [24] J. Hamann, S. Hannestad, G. G. Raffelt, G. G., and Y. Y. Wong, JCAP **09** 034 (2011).
 - [25] V. Barger, James P. Kneller, Hye-Sung Lee, Danny Marfatia, Gary Steigman, Phys. Lett. **B566**, 8 (2003).
 - [26] Doroshkevich, A. G.; Khlopov, M. Y., Soviet Astronomy Letters, **11**, 236 (1985) Translation Pisma v Astronomicheskii Zhurnal, **11**, 563 (1985).
 - [27] A. G. Doroshkevich, A. A. Klypin, and M. Y. Khlopov, Soviet Astron., **32**, 127 (1988).
 - [28] *Planck* Collaboration, Astron. & Astrophys. **594** A13 (2016).
 - [29] M. S. Smith, L. H. Kawano, and R. A. Malaney, Astrophys. J. Suppl. Ser. **85**, 219 (1993).
 - [30] Y. Xu, K. Takahashi, S. Gorieli, M. Arnould, et al., Nucl. Phys., **A918**, 61 (2013).
 - [31] K.A. Olive, G. Steigman, and T.P. Walker, Phys. Rep. **333**, 389 (2000).
 - [32] M. Yahiro, G. J. Mathews, K. Ichiki, T. Kajino, and M. Orito, Phys. Rev. **D65**, 063502 (2002).
 - [33] M. Orito, T. Kajino, G. J. Mathews and R. N. Boyd, Nucl. Phys., **A688**, 17c, (2001).
 - [34] A. Lewis, A. Challinor, and A. Lasenby, Astrophys. J., **538**, 473 (2000).
 - [35] A. Riess, et al. (*WMAP Collaboration*) Astrophys. J. *in Press*, (2016). arXiv:1604.01424
 - [36] G. Hinshaw, et al. (*WMAP Collaboration*) Astrophys. J. Suppl. Ser., **208**, 19 (2013).
 - [37] E. Aver, K. A. Olive and E. D. Skillman, arXiv:1503.08146 [astro-ph.CO].
 - [38] Y. I. Izotov, T. X. Thuan and N. G. Guseva, Mon. Not. Roy. Astron. Soc. **445**, 778 (2014).